

Impact Behavior Analysis of a Mechanical Monoleaflet Heart Valve Prosthesis in the Closing Phase

Gill-Jeong Cheon · K. B. Chandran*

= Abstract =

An analysis of the dynamics in the closing phase of the occluder of a mechanical monoleaflet heart valve prosthesis is presented. The dynamic analysis of the fluid in the vicinity of the occluder was based on the control volume approach. The backflow velocity of the fluid was computed by applying the continuity, Bernoulli's and momentum equations in the unsteady state. By considering the fluid pressure and gravity as external forces acting on the occluder, the moment equilibrium on the occluder was employed to analyze the motion of the occluder during closing and the force of impact between the occluder and the guiding struts. Occluder comes to rest after several oscillations in about 10–18 msec after the initiation of closing. As the aortic pressure increases, the occluder closes faster and comes to the final resting position earlier and the impact force increases also. But backflow is not affected by the variation of the aortic pressure. With decreasing time delay of the ventricle pressure, the occluder closes faster and impact force increases. The computed magnitudes of the occluder tip velocities as well as the backflow of the fluid during the closing phase using this model were in agreement with previously reported experimental measurements.

INTRODUCTION

The hemodynamic characteristics of the heart valve prostheses such as turbulent stresses and regions of relative stasis have been implicated in hemolysis, thrombosis, and resulting embolic complications. Numerous studies have been performed on the hemodynamics across prosthetic valves in the forward flow phase. Measurement of the velocity profiles and mechanical stresses

on the outflow side of the mechanical valves close to the occluders have demonstrated the existence of regions of flow reversal and stagnation as well as high turbulent shear stresses whose magnitudes may destroy red blood cells and platelets (Fatemi and Chandran, 1989; Yoganathan et al., 1986; Woo and Yoganathan, 1986). However, until recently, little attention have been directed to the understanding of the dynamics of valve closure and its effects on the design of the valves. With the advent of total artificial heart and incidences of structural failure of mechanical valves, incipience of cavitation bubbles at the instant of valve closure and subsequent collapse of the bubbles has been suggested as the reason for erosion of material on

〈접수 : 1992년 12월 30일〉

Department of Mechanical Engineering, Won-Kwang University, Iri city, Jeon-Buk, 570-749

* Department of Biomedical Engineering University of Iowa Iowa city, IA 52242 U.S.A.

the mechanical valves (Leuer, 1986; Young, 1989). At the instant of closure when the valve occluder impacts against the valve housing and the guiding struts, large positive and negative pressure spikes have been measured very close to the occluder in the outflow and inflow side of the valve respectively (Leuer, 1986; Lee et al., 1991). Such a large pressure difference may result in relatively high forces on the guiding struts and need to be considered in the design of the mechanical valves. Furthermore, a clearance is present between the occluder and the valve housing in order to provide flow in the vicinity of the valve during the portion of the cardiac cycle in which the valve is fully closed. It is believed that the presence of backflow will provide a smooth washout of blood in the periphery of the valve and minimize thrombus deposition in that region. However, the presence of large pressure spikes at the instant of valve closure may induce jet like flow through the clearance. Large mechanical stresses in this region may destroy platelets and induce thrombus deposition. The pressures within the clearance region and in the inflow side of the occluder may also fall below the vapor pressure of blood and may result in the incipience of cavitation bubbles.

More recently, number of studies have concentrated upon the flow dynamics in the vicinity of the occluders and in the clearance region with the valve in the fully closed position. Baldwin et al. (1991) measured the fluid velocities through the clearance and calculated the shear stress for a fully closed mechanical valve. Reif (1991) analyzed the mean velocity and maximum shear stress through the narrow slit formed by the closed leaflets of the bileaflet valve. Haggag(1990) calculated the shear stress induced by the leakage backflow of various valve prostheses. All of the above studies are concerned with the analysis of flow through

the clearance(leakage backflow) with the occluders in the fully closed position. Reif and Huffstutler(1985) analyzed the critical Reynolds number for the initiation of the occluder closing. They used Newton's second law of motion for rotating bodies and potential flow theory to mathematically model the closing process of a pivoting disc prosthetic valve. But divergence between theory and experiment occurred when the angle between the occluder and the housing was below 60° . They concluded that such a divergence was because of the limitation of the potential flow assumption.

An analysis of the dynamic behavior of the occluder during the valve closing phase is necessary to predict the closing backflow, occluder tip velocity, the relative velocity of the fluid against the occluder, and the force of impact of the occluder in the valve housing. In this paper, an analysis of the transient behavior of the occluder of a mechanical valve and the fluid is performed during the closing phase. This analysis considers the dynamics of the fluid in the vicinity of the occluder using a control volume approach. The equations of motion for the occluder include the moment equilibrium as the occluder rotates about a hinge point. The model used in this analysis is representative of a 29 mm tilting disc valve such as that of a Bjork-Shiley spherical disc valve.

METHOD OF ANALYSIS

The boundary of the control volume of the fluid used to analyze the flow dynamics during closing is depicted in Fig. 1 by dotted lines. For the convenience of analysis and computing, it was assumed that the flow is one dimensional in the axial direction. Because it is complicated to compute the projected area between a circular occluder and a circular orifice area at various

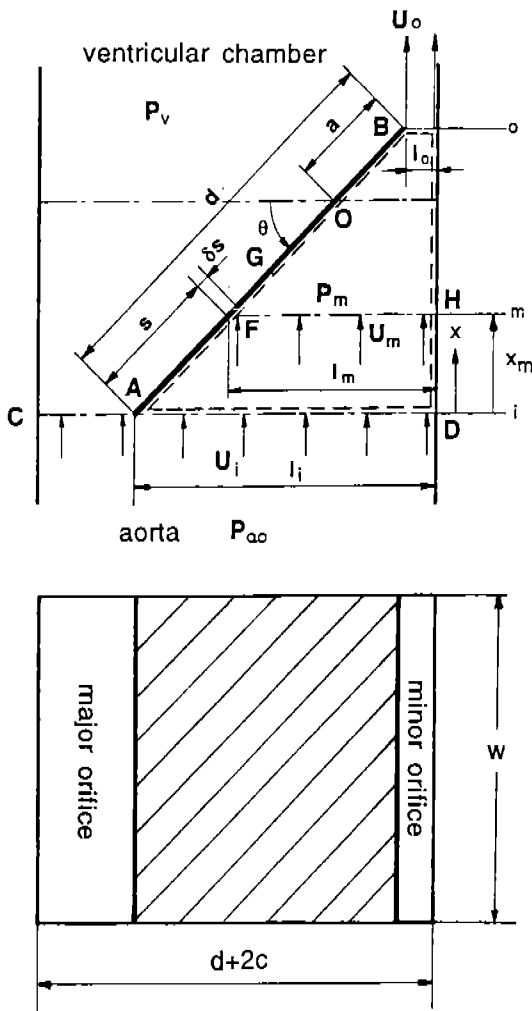


Fig. 1 Schematic diagram showing the control volume and the top view of the occluder : A, B; major and minor tip of the occluder, G; center of gravity of the occluder; O; pivoting point, d; occluder diameter, c; clearance between the occluder and the housing, w; occluder width, a; distance between the minor tip and the pivoting point, s; distance between the major tip and the discrete area, P_v , P_{a0} ; pressures in the ventricle and aorta, U_i , U_o ; inlet and outlet velocities

positions of the occluder during closing, the orifice and the occluder cross-sections were assumed as rectangular with depth w . It was also

assumed that the flow is laminar and velocity is uniform at every cross-section in the control volume as well as at the inlet. Thus, we are neglecting the effect of viscous diffusion in this short period. These assumptions make computation simple but give good results (Wipperman, 1985; Van Steenhoven and Van Dongen, 1979; Lee and Talbot, 1979). The backflow is separated into flows through the major and minor flow orifices at the entrance section 'i'. The analysis simulates the valve dynamics in the aortic position and it was assumed that the pressure of the fluid P_{a0} will be the same as that of the ventricle P_v when the fluid passes through the cross section 'CA' at the initiation of valve closing. It was also assumed that the pressure in the ventricular chamber is uniform. On the other hand, the fluid through section 'AD' passes through the converging channel between the occluder and the wall. Hence, velocities and pressures vary continuously through the converging channel. Because the control volume has moving boundaries and its shape vary according to time, unsteady conditions should be considered for the analysis. With the velocity u_i at the entrance section 'i', the velocity at the arbitrary section 'FH'('m') is expressed by using the unsteady continuity equation(Lu, 1979; White, 1986).

$$A_i(U_i - U_{ia}) - A_m(U_m - U_{if}) = dV_i/dt \quad (1)$$

$$U_{ia} = (d - a)\omega(\cos\theta) \quad (2)$$

$$U_{if} = (d - a - s)\omega(\cos\theta) \quad (3)$$

$$A_i = Wl_i, \quad A_m = Wl_m \quad (4)$$

$$V_i = (l_i + l_m)ws(\sin\theta)/2 \quad (5)$$

Where A_i , A_m , U_i , U_m and l_i , l_m are cross-sectional area, velocity and width at section 'i' and 'm', respectively. ω is the angular velocity of the occluder. U_{ia} and U_{if} are the axial velocity of the occluder at points 'A' and 'F'. 's' is the distance

from the leading edge 'A' to point 'F'. V_i is the volume contained between section 'AD' and 'FH'.

The unsteady Bernoulli's equation between section 'AD' and 'FH' is expressed as (Lu, 1979; White, 1986).

$$U_i^2/2 + p_i/\rho = U_m^2/2 + p_m/\rho + \int_0^x (\partial u/\partial t) dx \quad (6)$$

Where p_i and p_m are pressures at sections 'AD' and 'FH', respectively. ρ is the density of the fluid and x_m is the axial distance between section 'AD' and 'FH'. The pressure p_i at the entrance of the control volume is assumed to be always equal to the mean aortic pressure p_{ao} . Assuming the velocity U as the mean value between section 'i' and 'm', $\partial u/\partial t$ is expressed as

$$\partial u/\partial t = [(U_i + U_m)_t - (U_i + U_m)_{t-\delta t}] / (2\delta t) \quad (7)$$

The subscripts 't' and 't- δt ' represent the value at time 't' and 't- δt ' respectively, where ' δt ' is the time increment. Hence the third term of the right part of equation (6) is expressed as

$$\int_0^x (\partial u/\partial t) dx = [(U_i + U_m)_t - (U_i + U_m)_{t-\delta t}] s(\sin\theta) / (2\delta t) \quad (8)$$

The axial force F_p induced by the fluid pressure acting on the occluder is equal to

$$F_p = \int_0^d w p_m(\cos\theta) ds \quad (9)$$

F_p can be computed by adding all forces acting on small elements of width δs which are generated by dividing the occluder into a number of equal width strips in the direction parallel to the pivotal axis. F_p and δs can be expressed as

$$F_p = \sum_{m=1}^N w \delta s (\cos\theta) p_m \quad (10)$$

$$\delta s = d/N \quad (11)$$

Where N is the number of strips on the occluder.

Applying the unsteady momentum equation on the control volume with only one inlet and outlet (Fig. 2), following relationships are derived (Lu, 1979; White, 1986).

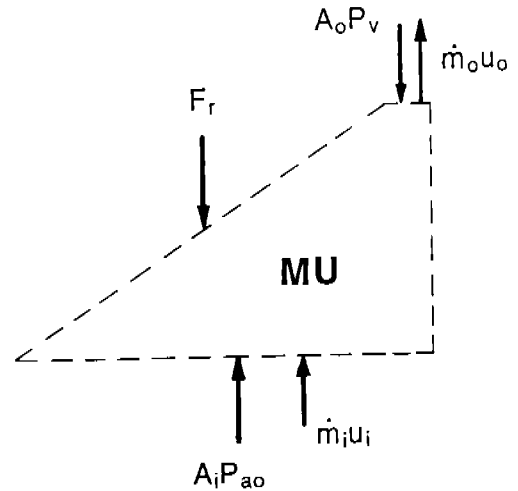


Fig. 2 Schematic diagram of the control volume for the momentum equation: A ; orifice area, U ; velocity, m ; mass flow rate, P ; pressure, M ; mass of the control volume, F_r ; reactional force

$$A_i P_{ao} - A_o P_v - F_r = m_o U_o - m_i U_i + d(MU)/dt \quad (12)$$

$$m_i = \rho A_i (U_i - U_{ia}) \delta t \quad (13)$$

$$m_o = \rho A_o (U_o - U_{ob}) \delta t \quad (14)$$

$$U_{ob} = -a\omega(\cos\theta) \quad (15)$$

$$U = (U_i + U_o)/2 \quad (16)$$

$$M = \rho w d (l_i + l_o) (\sin\theta)/2 \quad (17)$$

where U_b is the axial velocity of the occluder at point 'B', M is the mass of the control volume, U is the mean velocity of the control volume. F_r is the axial reaction force acting on the fluid control volume by the occluder. Equation(12) can be rearranged to express F_r as

$$F_r = A_p p_{a0} - A_o p_v + m_i U_i - m_o U_o - d(MU)/dt \quad (18)$$

By the principle of action and reaction, the two forces F_p and F_r should be equal.

$$F_p = F_r \quad (19)$$

If the velocity U_i at the entrance section is assumed, the velocity U_m at an arbitrary section 'm' is calculated from equation (1). By using equation(6), the pressure at section 'm' is calculated, and force F_p is obtained by equation (10). Applying assumed velocity U_i , F_r can be calculated by equation (18). If these values of F_p and F_r satisfy equation (19), the assumed velocity U_i is correct. But if these values do not satisfy equation (19), U_i should be modified through an iterative process as schematically depicted in Fig. 3 (step I).

The next step is to solve the governing equation of motion for occluder to determine the opening angle and the angular velocity of the occluder(Fig. 3, step II). Because of the stall condition, the lift force becomes zero when the occluder angle θ , is below 60° . If the opening angle becomes zero, there is no flow except between the clearance region and the occluder is subjected to only the fluid pressure. Hence, it is not appropriate to analyze the behavior of the occluder by applying the concept of lift force, and drag force similar to that employed in the analysis of the opening phase of the occluder (Cheon and Chandran, 1992; Reif et al., 1990). Therefore, the force by pressure and gravity are considered as external forces acting on the occluder in this analysis.

The governing equation of motion of the

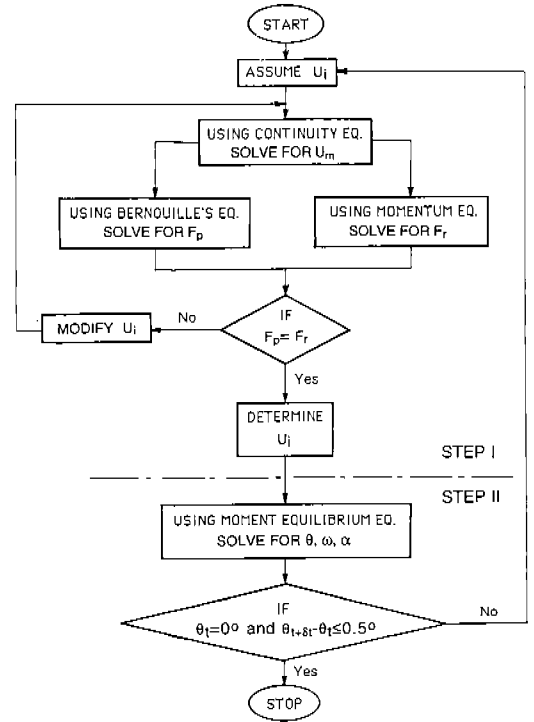


Fig. 3 Flow chart of the computational scheme

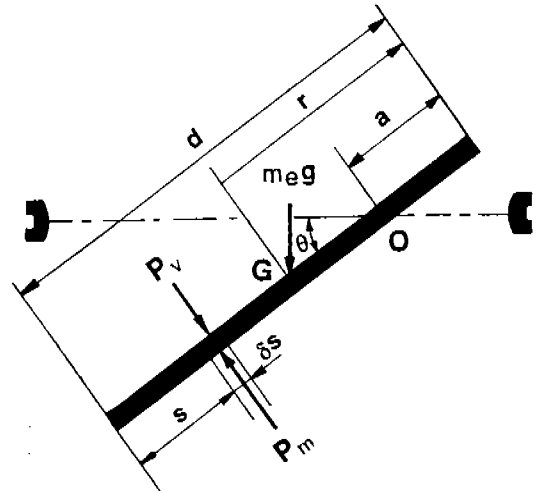


Fig. 4 Freebody diagram of the occluder: g ; acceleration of the gravity, m_e ; equivalent mass, P ; pressure, θ ; opening angle

occluder is expressed as follows(Fig. 4).

$$M_i = I_o (d^2\theta/dt^2) \quad (20)$$

where,

$$M_r = M_p + M_g \quad (21)$$

$$I_o = mr^2/4 + m(r-a)^2 \quad (22)$$

I_o is the mass moment of inertia of the occluder about the pivotal axis. M_p is the moment induced by pressure and M_g is the moment induced by the equivalent gravity. M_p and M_g are expressed as follows.

$$M_p = - \int_0^d (p_m - p_v) w(d-a-s) ds$$

$$= - \sum_{m=1}^N (p_m - p_v) w(d-a-s) \delta s \quad (23)$$

$$M_g = m_e g(r-a) (\cos\theta) \quad (24)$$

$$m_e = Ah(\rho_o - \rho) \quad (25)$$

where A and h are the area and thickness of the occluder, ρ_o is the density of the occluder. The initial conditions are specified as

$$\theta(0) = \theta_o \quad (26)$$

$$d\theta/dt(0) = 0 \quad (27)$$

$$d^2\theta/dt^2(0) = 0 \quad (28)$$

The backflow across the orifice is calculated by the relationship

$$Q_{nb} = A_{or} U_i \delta t \quad (29)$$

Where A_{or} is the orifice area. Since only the transient period of the occluder closure is considered in this analysis, backflow represents the amount of fluid flowing back into the ventricular chamber due to the closing motion of the occluder.

The occluder approaching the strut with an angular velocity ω_i impacts the strut during an extremely short time and will bounce from the struts with an angular velocity ω_2 (Fig. 5). The relation between angular velocities before and after impact is expressed as

$$\omega_2 = -e\omega_1 \quad (30)$$

Where 'e' is the coefficient of resilience. The an-

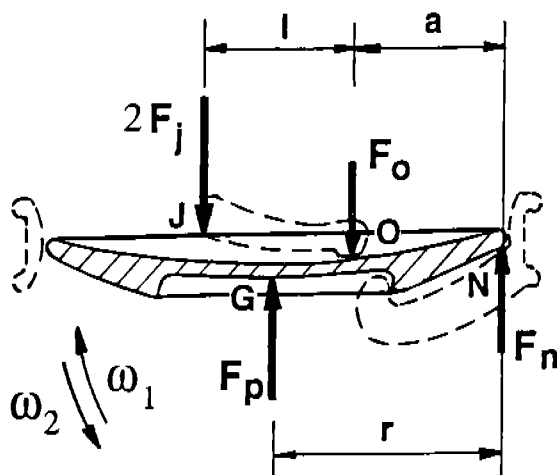


Fig. 5 Schematic diagram showing forces during impact: a ; distance between the minor tip and the pivoting point, l ; distance between the root of the inner strut and the pivoting point, r ; occluder radius, F_j ; force acting on the root of the inner strut, F_n ; force acting on the root of the outer strut, F_o ; force acting on the tip of the inner and outer strut, F_p ; force induced by fluid pressure, ω_1, ω_2 ; closing and opening angular velocities

gular acceleration α is expressed by the relationship

$$\alpha = d^2\theta/dt^2 = (\omega_2 - \omega_1)/t_i \quad (31)$$

Where t_i is the impact duration and is expressed as (Zukas et al., 1982)

$$t_i = 2.94 [5 / (4Mn'v^{1/2})]^{2/5} \quad (32)$$

Where,

$$M = 1/m_i + 1/m_t \quad (33)$$

$$n^1 = 16(C_R/\zeta^3)^{1/2} [3\pi(k_i + k_t)] \quad (34)$$

$$k_i = (1 - \nu_i^2)/\pi E_i, k_t = (1 - \nu_t^2)/\pi E_t \quad (35)$$

$$1/C_R = 1/R_{im} + 1/R_{tm} + 1/R_{iM} + 1/R_{tM} \quad (36)$$

In these equations, m , E and ν are mass, Young's modulus, and Poisson's ratio, respectively. The subscripts 'i' and 't' refer to the impactor and the target. In this case, they refer to the

Table 1 Values of η and ζ defined in equations (34) and (37)

η	0	10°	20°	30°	40°	50°	60°	70°	80°	90°
ζ	—	0.851	1.220	1.453	1.637	1.772	1.875	1.987	1.994	2.00

occluder and the strut, respectively. 'v' is the approaching velocity of the occluder. R_{im} , R_{iM} are principal radii of curvature of the occluder and R_{tm} , R_{tM} are principal radii of the contacting points of the struts. ' ζ ' is a function of radius of curvature and is given in Table 1 as a function on η (Zukas et al., 1982), where

$$\eta = \arccos\{C_R[(1/R_{im}-1/R_{iM})^2 + (1/R_{tm}-1/R_{tM})^2 + 2(1/R_{im}-1/R_{iM})(1/R_{tm}-1/R_{tM})(\cos 2\phi)]^{1/2}\} \quad (37)$$

where ϕ is the angle between normal planes containing curvatures $1/R_{im}$ and $1/R_{tm}$. When occluder closes completely, it will touch the two roots of the inlet strut at point 'J', and the root of the outlet strut at point 'N'. If the impact durations at points 'J' and 'N' are different, the longer value will be used in calculating α . The rotational and linear equilibrium equations of the occluder are expressed as

$$2F_j - F_p(r-a) + F_n a = I_o \alpha \quad (38)$$

$$F_o + 2F_j - F_p - F_n = m(r-a)\alpha \quad (39)$$

Where F_o , F_j and F_n are reactional impact forces at point 'O', 'J' and 'N'. F_p is the force by fluid pressure. There are three unknowns F_o , F_j and F_n , but there are only two equations. To solve this problem, the worst case was assumed with F_o set equal to zero. The inlet strut acts like a cantilever and will tend to deflect. By geometrical compatibility, the strain will increase as the distance from the hinge point 'O' increases. Hence the magnitude of F_o will be much less than that of F_j and F_n . The larger one of the two forces F_j and F_n will be the maximum impact load acting on the occluder. As shown in

step II of Fig. 3, the equilibrium equations along with the initial conditions are employed to compute the angular acceleration, occluder tip velocity and force of impact of the occluder.

RESULTS AND DISCUSSION

Transient behavior was analyzed from the beginning of the closing motion until the end of fluttering of the occluder after impacting against the guiding struts. To analyze the transient behavior during the short duration of the closing of the occluder, the time increment δt was selected as 0.1 msec. The convergence criterion specified was that the computed velocities were correct if the difference between F_i and F_p was less than or equal to 0.005 N which is equal to about 0.1% of the force of the static pressure(Fig. 3). With the smaller angles less than 5°, the occluder is very close to the final closed position with very small clearance(about 0.07mm) between the occluder and the housing. Hence, for angle of opening less than 5°, we assumed that the relative velocity of the fluid in the control volume is zero. Time 't' was selected to be zero at the moment when backflow is initiated and it was assumed that the initial velocity of the fluid is zero. The occluder was divided into 24 strips of equal width in these computations. The governing equations of motion for the occluder were solved by 4th order Runge-Kutta method. Heart rate and cardiac output were selected to be 70 beats per minute(bpm) and 1.0×10^{-4} m³/sec (6L/min), respectively. Ventricular pressure was assumed to decrease from a value equal to the aortic pressure(when the valve is fully open) to zero with a time delay T_d .

T_d was varied between 0 and 0.03 sec. The average aortic pressure at closing was varied between 10.7–16.0 kPa (80–120 mmHg) and was assumed to be constant during closing. For the terminal condition for step II of Fig. 3, the occluder was assumed to have reached the resting position when the occluder angle of the successive time increment is less than 0.5° after impact. Valve dimensions and various parameters are listed in Table 2.

Table 2 Various parameters and valve dimensions used in this study

Parameter	Value	
a	0.006	m
A	0.00045	m ²
A_{or}	0.00046	m ²
c	0.00005	m
d	0.024	m
e	0.5	
h	0.0015	m
r	0.012	m
w	0.019	m
θ_{max}	70°	
ρ	1060	kg/m ³
ρ_o	2480	kg/m ³

a; distance from the pivotal axis to the leading edge, A; occluder area, A_{or} ; orifice area, c; clearance between the occluder and the housing, d; occluder diameter, e; resilience coefficient, h; idealized occluder thickness, r; occluder radius, w; idealized width of the occluder, θ_{max} ; maximum opening angle, ρ ; density of the fluid, ρ_o ; density of the occluder

Angle between the occluder and the housing as a function of time at various T_d are plotted in Fig. 6 for the case at the aortic pressure, P_{ao} of 13.3 kPa(100 mmHg). It takes about 10–18 msec before the occluder comes to rest in the fully closed position from the initiation of the closing. With decreasing T_d (larger rate of decrease of the ventricle pressure to zero), the

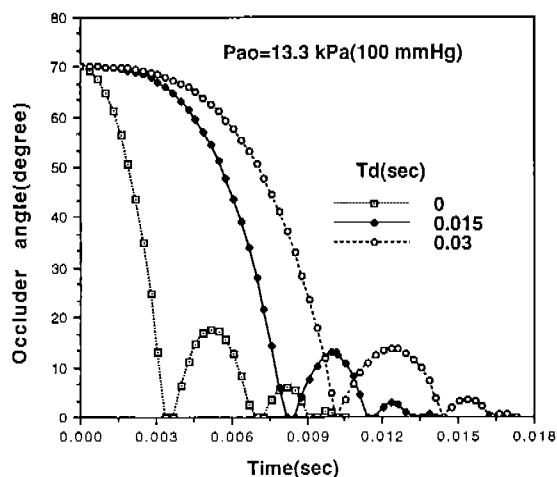


Fig. 6 Angle between the occluder and the valve housing (θ) as a function of time for $P_{ao}=13.3$ kPa (100 mmHg)

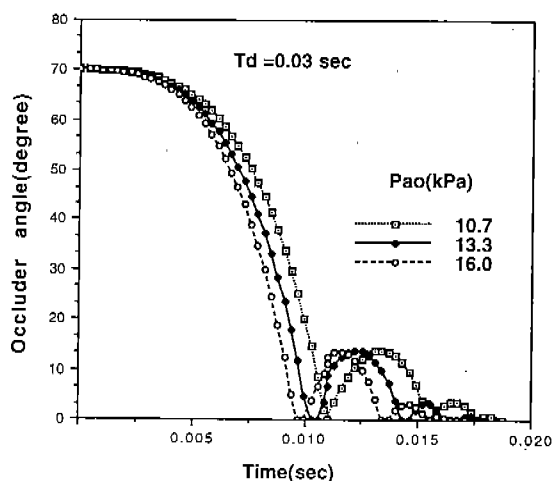


Fig. 7 Angle between the occluder and the valve housing (θ) as a function of time for $T_d=0.03$ sec

occluder closes faster and comes to the final resting position earlier. In the normal human ventricle, the time delay for the ventricle pressure to reduce to zero is about 0.03 sec (Guyton, 1971).

Fig. 7 shows the occluder angle as a function of time at various aortic pressures for the case

when $T_d=0.03$ sec. As the aortic pressure increases, the occluder closes faster. The first impact occurs after about 10 msec from the initiation of the closing and occluder comes to the resting position after about 16–18 msec.

Velocity of the occluder tip at the major orifice is plotted in Fig. 8 for the case when $P_{a0}=13.3$ kPa(100 mmHg). The maximum velocity of the occluder tip is in the range of 8–15 m/sec. Guo and Hwang(1990) have reported that the maximum velocity of the occluder tip of a bileaflet valve is about 4.5–4.8 m/sec. The dimension of the occluder of the monoleaflet valve is longer than that of the bileaflet valve. Since the moment arm is larger, the calculated tip velocities for the monoleaflet valve are larger than those measured for the bileaflet valve and appear to be reasonable. These values are much higher than the tip velocities of 0.65–1.42 m/sec computed during the opening phase (Cheon and Chandran, 1992). Gross et al. (1991) have reported that the fluid velocity should be over 13 m/sec to induce cavitation at the atmospheric pressure, and concluded that cavitation will not occur with mechanical valves. However presence of cavitation bubbles have been reported with mechanical valves in an artificial ventricle (Stinebring et al., 1991; Graf et al., 1991). The velocity of the fluid attached to the surface of the occluder should be the same as that of the occluder itself. Hence even though the mean velocity measured by velocimeter may be lower than the critical value, cavitation might be induced by the fluid attached at the occluder surface. Stinebring et al. (1991) also have reported that cavitation bubbles are observed in the major orifice region and not in the minor orifice region. It might be due to the fact that the occluder tip velocity in the minor orifice is only 1/3 of that in the major orifice due to the shorter moment arm.

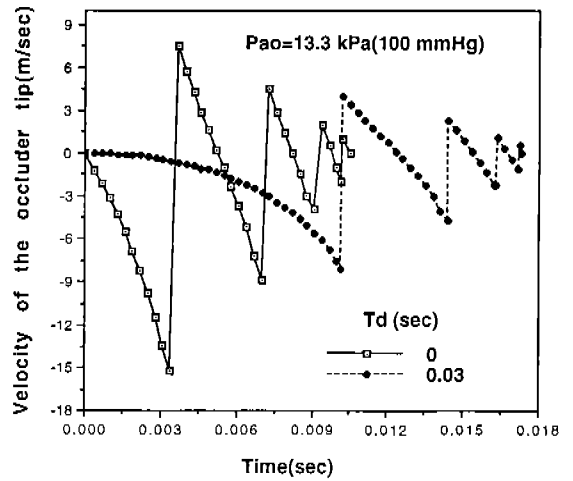


Fig. 8 Velocity of the occluder tip at the major orifice as a function of time for $P_{a0}=13.3$ kPa (100 mmHg)

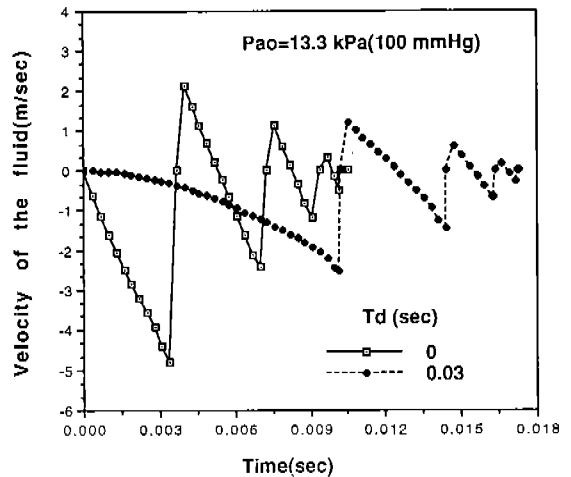


Fig. 9 Velocity of the fluid as a function of time for $P_{a0}=13.3$ kPa(100 mmHg)

Fig. 9 shows the fluid velocity in the major orifice for the case when $p_{a0}=13.3$ kPa(100 mmHg). With $T_d=0.03$ sec, the maximum backflow velocity approaches a magnitude of 2.5 m/sec. The fluid in this region oscillates during closing and the flow profile is very similar to the major tip velocity profile.

Fig. 10 shows the relative velocity of the fluid

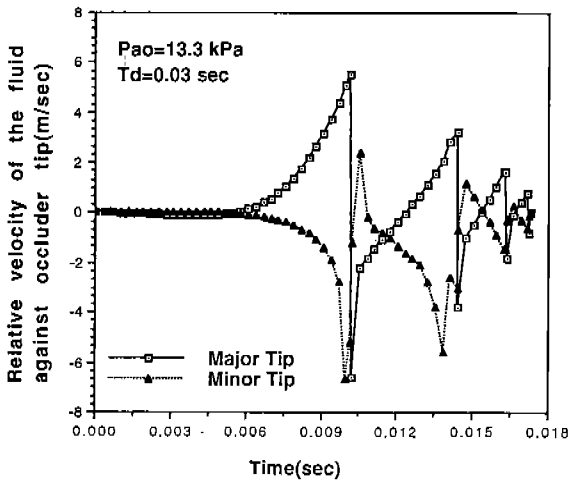


Fig. 10 Relative velocity of the fluid against the occluder tip for $P_{ao}=13.3$ kPa (100 mmHg), $T_d=0.03$ sec

against the occluder tip for the case when $p_{ao}=13.3$ kPa (100 mmHg) and $T_d=0.03$ sec. The maximum value is determined at the initial valve closure and is about 6–7 m/sec.

Fig. 11 shows the closing backflow as a function of time for the case when $T_d=0.03$ sec. The backflow also exhibit oscillations similar to that of the occluder, but the net backflow volume is about 4 cc, and this value does not change with various values of P_{ao} . Sabbah and Stein(1984) have measured the closing backflow to be about 3 cc and reported that the backflow does not vary with the mean aortic pressure. In their experiments, they used a Bjork-Shiley valve with orifice diameter of 0.0222m. Because the diameter of the orifice used in this analysis is 0.024m, the calculated closing backflow appears to be very reasonable.

The maximum impact force between the occluder and the struts occurs at point 'J', and it is shown in Fig. 12 for the case when $p_{ao}=13.3$ kPa (100 mmHg). It was assumed that the resilience coefficient e is 0.5, elastic modulus and Poisson's ratio of the struts and occluder

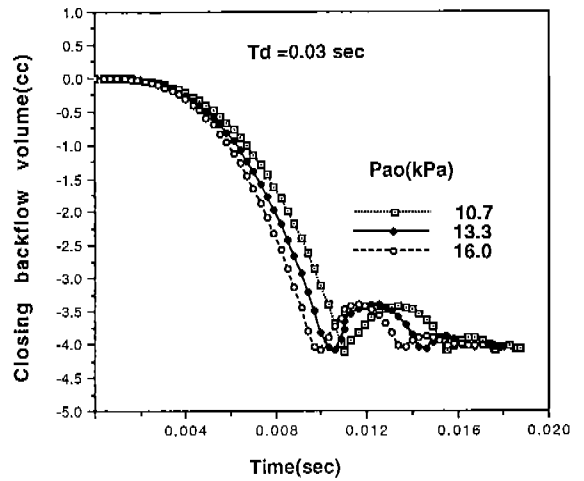


Fig. 11 Closing backflow volume as a function of time

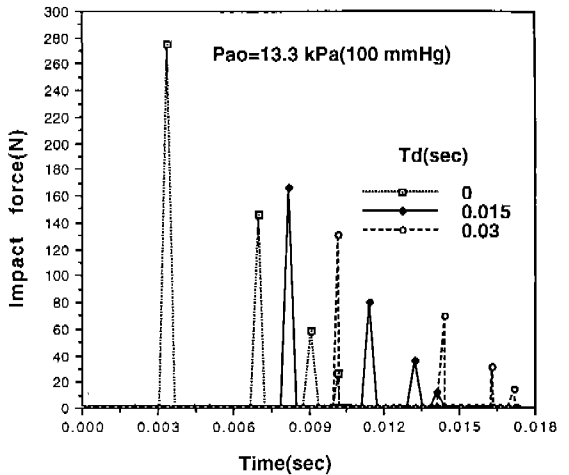


Fig. 12 Impact force between the occluder and the strut during the transient closing phase for $P_{ao}=13.3$ kPa (100 mmHg)

were assumed as 209 GN/m², 0.3 and 27.6 GN/m², 0.23, respectively. To satisfy surface contact, the surfaces of the contacting areas of the struts might be machined to have equal radius of curvature with that of the occluder. With this assumption, all principal radii of curvature were assumed to be 0.1m and angle ϕ was assumed to be 0°. The maximum impact force occurs at

the first impact and are in the range of 140–280 N. Impact duration is in the range of 35–45 μ sec.

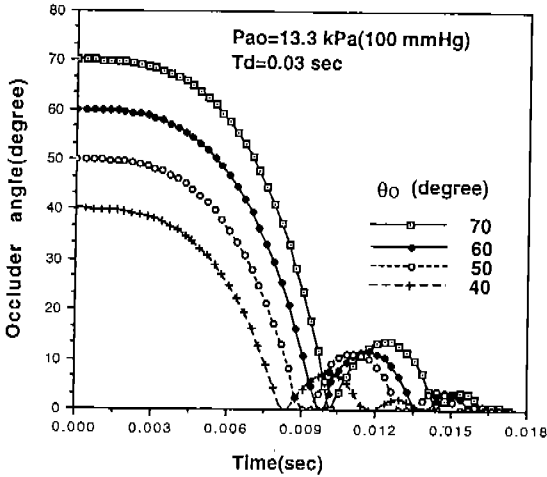


Fig. 13 Angle between the occluder and the valve housing(θ) as a function of time for $P_{ao}=13.3$ kPa(100 mmHg), $T_d=0.03$ sec

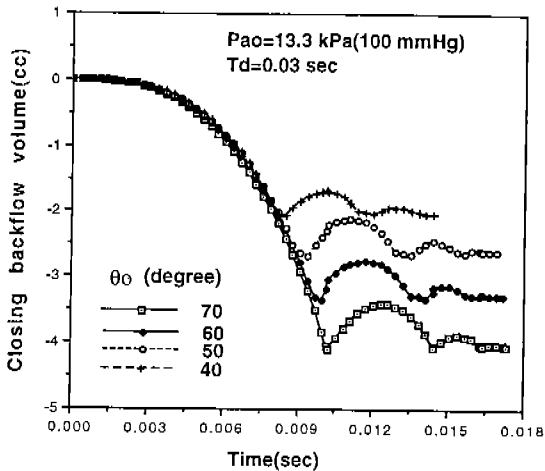


Fig. 14 Closing backflow volume as a function of time for $P_{ao}=13.3$ kPa(100 mmHg), $T_d=0.03$ sec

Fig. 13 and Fig. 14 show the plots of occluder angle and backflow volume, respectively, for the case when $p_{ao}=13.3$ kPa (100 mmHg) and

$T_d=0.03$ sec for various initial opening angle of the occluder. As the initial opening angle decreases, the backflow decreases. With smaller opening angles, the occluder will reach the fully closed position earlier and will displace less amount of fluid to the ventricular chamber resulting in smaller closing backflow as would be expected.

CONCLUSION

In this analysis, transient behavior of mechanical monoleaflet valve was analyzed during the closing phase. The fluid contained in the converging volume between the occluder and the wall was considered as a control volume and the flow was assumed to be laminar and one dimensional. Applying the continuity, Bernoulli's and momentum equations, the closing backflow volume and its velocity were calculated. The backflow volumes are in the range of 1.5–4.1 cc with various initial opening angles. As the initial opening angle decreases, the backflow volume decreases. The maximum backflow velocities are in the range of 3–5 m/sec. The position of the occluder as a function of time and the tip velocity were calculated by solving the governing equations of motion with the fluid pressure and equivalent gravitational force as external forces. Occluder comes to rest after several oscillations in about 10–18 m/sec after the initiation of closing. Impact forces between the occluder and the struts were estimated and the maximum impact forces occur at the first impact and are in the range of 140–280 N. Impact durations between the occluder and the struts are in the range of 35–45 μ sec. It was also possible to calculate the relative velocity of the fluid against the occluder tip. The maximum values are in the range of 6–7 m/sec.

The calculated values of the tip velocity and

backflow volume are in agreement to those of the previously reported experimental results. Hence, the theoretical analysis employed in this study appears to be reasonable. The results of this study may be extended for the analysis of cavitation, mechanical stresses on the formed elements as well as to estimate the endurance limit of the prosthetic valve. And these results can be applied to determine the optimal dimensions and shapes of the struts to minimize the impact forces. Water hammer effect neglected in this study will affect the behavior of the occluder after first impact, and it should be analyzed in the future study.

ACKNOWLEDGEMENTS

Support by funds from KOSEF(Korea Science and Engineering Foundation) for Gill-Jeong Cheon's research at the university of Iowa is gratefully acknowledged.

REFERENCES

- 1) Baldwin J.T., Tarbell J.M., Deutsch S., Geselowitz D.B., 1991, "Mean Velocities and Reynolds Stresses Within Regurgitant Jets Produced by Tilting Disc Valves", *ASAIO Transactions*, Vol. 37, pp. 348-349
- 2) Cheon G.J., Chandran K.B., 1992, "Dynamic Behavior Analysis of Mechanical Monoleaflet Heart Valve Prostheses in the Opening Phase", *Proceedings of the ASME Winter Annual Meeting. BED-Vol. 22*, pp. 423-426 : and to be published in *ASME J. of Biomchanical Engineering* (1993).
- 3) Fatemi R., Chandran K.B., 1989, "An In Vitro Comparative Study of St. Jude Medical and Edwards-Duromedics Bileaflet Valves Using Laser Anemometry", *ASME J. of Biomechanical Engineering*, Vol. 111, pp. 298-302
- 4) Graf T., Fisher H., Reul H. Rau G., 1991, "Cavitation Potential of Mechanical Heart Valve Prostheses", *The International Journal of Artificial Organs*, Vol. 14, pp. 169-174
- 5) Gross J.M., Guo G.X., Hwang N.H.C., 1991, "Ventricular Pressure Cannot Cause Cavitation in Mechanical Heart Valve Prostheses", *ASAIO Transactions*, Vol. 37, pp. 357-358
- 6) Guo G.X., Xu C.C., Hwang N.H.C., 1990, "Laser Assessment of Leaflet Closing Motion in Prosthetic Heart Valves", *J. of Biomedical Engineering*, Vol. 12, pp. 477-481
- 7) Guyton, 1971, "Textbook of Medical Physiology", W.B.Saunders Co., Philadelphia, 4th ed., p. 153
- 8) Haggag Y.A.M., 1990, "A Comparative Study of the Shear Stress Induced in the Leakage Backflow Produced by Four Types of Heart Valve Prostheses", *IMEchE J. of Engineering in Medicine*, Vol. 204, pp. 111-114
- 9) Lee C.S., Clausen J.D., Chandran K.B., 1991, "Flow Dynamics in the Disc Clearance Region of a Bileaflet Mechanical Heart Valve Prosthesis During the Closing Phase", *Proceeding of 3rd USA-China-Japan Conference on Biomechanics*, Georgia Institute of Technology, Atlanta, Georgia, pp. 137-138
- 10) Lee C.S.F., Talbot L., 1979, "A Fluid-mechanical Study of the Closure of Heart Valves", *J. of Fluid Mechanics*, Vol. 91, Part 1, pp. 41-63
- 11) Leuer L., 1986, "In Vitro Evaluation of Drive Parameters and Valve Selection for the Total Artificial Heart", presented at Annual Meeting of the Canadian Council of Cardiovascular Perfusionists
- 12) Lu P.C., 1979, "Fluid Mechanics", The

- Iowa State University Press, pp. 287-293
- 13) Reif T.H., Huffstutler M.C., 1985, "A Note on the Critical Flow to Initiate Closure of Pivoting Disc Mitral Valve Prostheses", *J. of Biomechanics*, Vol. 18, pp. 151-156
 - 14) Reif T.H., Schulte T.J., Hwang N.C.H., 1990, "Estimation of the Rotational Undamped Natural Frequency of Bileaflet Cardiac Valve Prostheses", *ASME J. of Biomechanical Engineering*, Vol. 112, pp. 327-332
 - 15) Reif T.H., 1991, "A Numerical Analysis of the Backflow Between the Leaflets of a St. Jude Medical Cardiac Valve Prosthesis", *J. of Biomechanics*, Vol. 24, pp. 733-741
 - 16) Sabbah H.N., Stein P.D., 1984, "Comparative Study of the Amount of Backflow Produced by Four Types of Aortic Valve Prostheses", *ASME J. of Biomechanical Engineering*, Vol. 106, pp. 66-71
 - 17) Stinebring D.R., Lamson T.C., Deutsch S., 1991, "Techniques for in-vitro Observation of Cavitation in Prosthetic Heart Valves", *ASME Cavitation and Multiphase Flow Forum*, pp. 119-124
 - 18) Van Steenhoven A.A., Duppen Th. J.A.G., Cauwenberg J.W.G., 1982, "In Vitro Closing Behaviour of Bjork-Shiley, St. Jude and Hancock Heart Valve Prostheses in Relation to the in-vivo Recorded Aortic Valve Closure", *J. of Biomechanics*, Vol. 15, pp. 841-848
 - 19) Van Steenhoven A.A., Van Dongen M.E. H., 1979, "Model Studies of the Closing Behaviour of the Aortic Valve", *J. of Fluid Mechanics*, Vol. 90, pp. 21-32
 - 20) White F.M., 1986, "Fluid Mechanics", McGraw-Hill Book Co., 2nd ed., pp. 113-155
 - 21) Wipperman F.K., 1985, "On the Fluid Dynamics of the Aortic Valve", *J. of Fluid Mechanics*, Vol. 159, pp. 487-501
 - 22) Woo Y.R., Yoganathan P.Y., 1986, "In Vitro Pulsatile Flow Velocity And Shear Stress Measurements in the Vicinity of Mechanical Mitral Heart Valve Prostheses", *J. of Biomechanics*, Vol. 19, pp. 39-51
 - 23) Yoganathan A.P., Woo Y.R., Hsu W.S., 1986, "Turbulent Shear Stress Management in the Vicinity of Aortic Valve Prostheses", *J. of Biomechanics*, Vol. 19, pp. 433-442
 - 24) Young F.R., 1989, "Cavitation", McGraw-Hill Book Co., pp. 265-290
 - 25) Zukas J., Cholas T., Swift H.F., Greszczuk L.B., Curran D.R., 1982, "Impact Dynamics", John Wiley & Sons, pp. 57-70